NeuroImage 47 (2009) T154–T162

Contents lists available at ScienceDirect

NeuroImage

journal homepage: www.elsevier.com/locate/ynimg

Infrared thermal imaging: A review of the literature and case report

Babak Kateb [a,b,*], Vicky Yamamoto [d], Cheng Yu [a], Warren Grundfest [b,c], John Peter Gruen [a]

[a] Department of Neurological Surgery, University of Southern California, Keck School of Medicine, Los Angeles, CA, USA
[b] Brain Mapping Foundation and International Brain Mapping and Intraoperative Surgical Planning Society, Santa Monica, CA, USA
[c] UCLA School of Medicine, Department of Surgery, Los Angeles, CA, USA
[d] Eli and Edythe Broad Center for Stem Cell and Regenerative Medicine, USC-Keck School of Medicine, Los Angeles, CA, USA

ARTICLE INFO

Article history:
Received 25 January 2009
Revised 14 March 2009
Accepted 18 March 2009
Available online 28 March 2009

Keywords:
Brain tumor
Brain tumor imaging
Brain tumor biophotonic
Thermal imaging
Infrared imaging
Intraoperative imaging
Image-guided surgery
Brain Metastasis
Melanoma
Multi-Modality Imaging

ABSTRACT

Intraoperative Thermal Imaging (ITI) is a novel neuroimaging technique that can potentially locate the margins of primary and metastatic brain tumors. As a result, the additional real-time anatomical and pathophysiological information may significantly contribute to an improved extent of tumor resection. Our objectives in this article are i) to briefly discuss the current status of intraoperative imaging modalities including ITI and ii) to present a case report that evaluates the usefulness of ITI in detection of brain tumor and its margins. In this case report, ITI was used in a patient with a metastatic intracortical melanoma. The thermal profile of the tumor and surrounding normal cerebral cortex were mapped with a ThermaCAM P60 (TCP60) infrared camera by FLIR Systems. The data obtained by TCP60, intra-operatively, revealed a clear demarcation of tumor with significant temperature differences, up to 3.3 °C, between the tumor core (36.4 °C) and the surrounding normal tissue (33.1 °C). Ultrasound and pre-resection MR and CT confirmed the position and size of the metastasis. The volume of the tumor was preoperatively calculated using the CyberKnife™ software and postoperative volumetric measurement of the tumor residual was calculated by the Gamma Knife™ software. Our result, along with previously published results of others, suggests that thermal imaging could be used to provide a rapid, non-invasive, and real-time intra-operative imaging.

Introduction

Despite considerable advances in diagnosis and treatment, the survival rate of patients with malignant brain tumors has not significantly improved. The mortality from malignant brain tumors remains high, as the median survival rate is 12 to 18 months in patients with glioblastoma and 41 months in patients with anaplastic astrocytomas (Wen and Kesari, 2008; Stupp et al., 2006; Mitchell et al., 2005; DeAngelis, 2001). Surgical resection followed by radiotherapy and chemotherapy offers a survival benefit, particularly when resection is complete (Sanai and Berger, 2008; Mitchell et al., 2005; Nazzaro and Neuwelt, 1990; Mineo et al., 2002; Laws et al., 2003). Despite all advances made in the field of brain imaging in the last decades, brain shift, also known as post-imaging brain distortion, often makes intraoperative delineation of the tumors difficult as its preoperative imaging can no longer be fully relied on (Reinertsen et al., 2007; Nabavi et al., 2001; Hill et al., 1998; Knauth et al., 1999). Moreover, it is difficult to distinguish brain tumors from normal surrounding tissue if they exhibit infiltrative nature, which makes it virtually impossible to achieve near total resection. Intraoperative multi-modality imaging can be helpful in resolving these issues, and thus in increasing the extent of resection. Therefore, there is a great need for development and integration of new intra-operative brain imaging/mapping technologies such as thermography. Many of these technologies are currently available for research purposes and have been shown to hold a great promise in assisting surgeons to achieve near total resection through a more objective detection and up-to-date delineation of the tumor margins.

Background

Brief history and current state of thermal imaging

Human body temperature distribution is influenced by many complex factors; the heat exchange processes between skin tissues, metabolic activity, vasculature, circadian rhythm, and the regulating of the sympathetic and parasympathetic activity for maintaining homeostasis (Merla and Romani, 2006; Saxena and Willital, 2008). A presence of disease often alter the homeostasis, hence thermobiological diagnosis has been used as one of the important diagnostic

* Corresponding author. Department of Neurological Surgery, University of Southern California, Keck School of Medicine, Los Angeles, CA, USA
E-mail address: bkateb@bimisps.org (B. Kateb).

1053-8119/$ – see front matter © 2009 Elsevier Inc. All rights reserved.
doi:10.1016/j.neuroimage.2009.03.043

measurements, as the first documented use of it can be found in the writings of Hippocrates (circa 480 BC) (Jiang et al., 2005; Samaras and Greenblatt, 1983).

Thermal, or infrared, energy is the part of electromagnetic radiation that an observer perceives as heat. Infrared thermography allows us to visualize temperature distribution of the human body and has been used in medical practice since the 1950s. The earliest modern thermography was used to screen breast tumor, although due to the drawback of less-sensitivity and low resolution, it is now mainly used as an alternative method to detect breast tumor mass (Barrett et al., 1980; Head et al., 2000). Effort has been made by many researchers to improve accuracy of tumor detection by increasing resolutions of cameras, formulating better algorithm, and producing more sophisticated instruments (Mital and Scott, 2007; Gonzalez, 2007; Arora et al., 2008).

Although thermoimaging has been used extensively and is well established in aerospace, military and industry, its use in the medical setting is still under investigation, with the exception of breast tumor screening. Thermoimaging has potentially broad applications in practical and experimental medicine, as many clinicians and scientists have recently published exciting new reports covering a wide range of medical specialties. Among the examples are the use of thermal imaging for the monitoring and assessment of renal ischemia (Gorbach et al., 2003, 2008), surface blood flow and local thermodynamics during surgery in patients with moyamoya disease (Nakagawa et al., 2008) and viability of gastric tube during esophagectomy (Nishikawa et al., 2006). Thermography is also used in determining the location of sensory motor cortex during surgery by measuring cortical surface temperature after median nerve stimulation. A slight temperature increase after the stimulation of thalamic cortical tract was elicited by metabolic activity and heating the sensory cortex following neuronal activity (Ueda et al., 1997).

Functional mapping using thermoencephaloscopy (TES) was documented in 1990 by Shevelev and coworkers in which changes on IR radiation were measured through intact skull of rats. TES has been utilized for many years to detect areas of hyperthermia in functional imaging and brain mapping and to study associative learning, movement, and sleep (Gorbach, 1993; Shevelev, 1992, 1998). This method was non-invasive and had a reasonable spatial and temporal resolution. The pitfalls of this method were a failure to separate cerebral blood flow (CBF) and metabolic events as well as limited resolution of imaging instruments (Shevelev, 1992, 1998; Shevelev et al., 1993).

In 2008,Saxena and Willital (2008) reported on the use of infrared thermography in pediatric cases. 483 examinations on 285 patients showed that thermoimaging could recognize abnormal temperature distributions on skin surface caused by hemangiomas, vascular malformations, varicoceles, extremity thrombosis, abscess, sternal wound infections, gangrene, and other symptoms/disorders. The authors concluded from the collection of 10 years of data that thermoimaging is proven to be a very valuable, quick, cost-efficient, and non-invasive way to identify or to verify clinical states and therefore used as an effective diagnostic parameter in the pediatric age group.

Current state of intraoperative diagnostics for brain tumor other than ITI

The loss of cerebrospinal fluid, tumor resection, edema, and placing surgical apparatus during surgery can often contribute to the "brain shift" phenomenon, causing significant inconsistencies with preoperative imaging. However, recent advances in intraoperative biomedical imaging such as CT and MRI scans have greatly improved our effort to identify tumors and delineate their margins. One such technological advance is the use of intraoperative Magnetic Resonance Imaging (iMRI) in the operating room, which was first introduced by Dr. Peter Black and his colleagues (Schulder and Carmel, 2003; Black et al., 1997). At present, this technology offers surgeons the best intraoperative image guidance during brain tumor resection as it provides various surgically relevant parameters such as location of the tumor and its borders, as well as functional, metabolic and vascular parameters at the highest resolution (Mittal and Black, 2006; Fahlbusch and Samii, 2007). The use of iMRI can detect brain shift, which greatly maximizes tumor resections and helps avoid harmful resection of normal tissues and critical structures (Frangioni, 2008; Tempany and McNeil, 2001). However, its use creates challenges for surgeons and operating room (OR) staff, such as the size of the equipment to be placed in the OR, maintaining sterility and MR-compatible surgical instruments. In an attempt to overcome some of these challenges, Black et al. (1997) constructed a specialized OR. Others integrated MRI suites in the OR that can be transformed into sterile surgical areas or designed a compact, portable MRI (Hall et al., 2000; Hadani et al., 2001; Schulder et al., 2001; Hall and Truwit, 2008). Nevertheless, the cost of the iMRI remains high and using the procedure can prolong the operating time as each scan takes about 20 min (Fahlbusch and Samii, 2007). Therefore, it is imperative to explore faster and more cost-efficient non-invasive alternatives to iMRI.

Aside from iMRI, there are reports of intraoperative imaging utilizing computer tomography and ultrasound, in an attempt to improve maximum brain tumor resection. For instance, Nakao et al. (2003) used a mobile CT which is readily available in an operating room to acquire intraoperative images during tumor resection. Intra-operative 3D ultrasound is another emerging alternative intraoperative modality that scientists and clinicians are exploring. Intraoperative 3D ultrasound (3D-iUS) is proven to be excellent in capturing images of metastasis, meningeoma and angioma over those in malignant glioma and can detect brain shifting (range: 2–25 mm) (Lindner et al., 2006; Unsgaard et al., 2006). Recently, Rasmussen et al. (2007) reported neuronavigation utilizing intraoperative 3D ultrasound that integrate preoperative structural and functional MR data as well as diffusion tensor imaging data to correct brain shift in twelve patients. They demonstrated that automatic brain shift correction using the method was feasible, and were able to optimize surgical planning successfully. Both CT and ultrasound imaging modalities allow surgeons to obtain several updates during surgery and thus are able to minimize the problem associated with brain shift during an operation. However, the resolution of CT and ultrasound imaging is still inferior to iMRI and their ability to delineate tumor border remains unsatisfactory (Fahlbusch and Samii, 2007).

Current state of intraoperative thermal imaging in brain tumors

Although not as common as intraoperative MRI, there are several experimental models and case reports utilizing thermal imaging in brain tumor detection. In both animal and human models, primary brain tumors of glial origins consistently have lower temperature than the surrounding normal tissue (Gorbach et al., 2004; Ecker et al., 2002; Papaioannou et al., 2002; Konerding et al., 1998), which is consistent with the earlier study using human model by Koga et al. (1987). Papaioannou et al. (2002) reported a C6 glioma mouse model with 0.3–0.7 °C temperature difference. The temperature was lower at the center of the tumor, with the difference growing larger as the tumor growth progresses. In patients, Gorbach et al. (2004) showed that brain tumors of glial origin generally have 0.5–2.0 °C difference (lower) compared to normal surrounding tissue. Similar cases were reported by Ecker et al. (2002), where 11 out of 14 primary tumors were hypothermic. Both Papaiannou and Gorbach also reported delayed recovery of temperature in tumors after irrigation of the tumor surface with cold saline (Papaioannou et al., 2002; Gorbach et al., 2004).

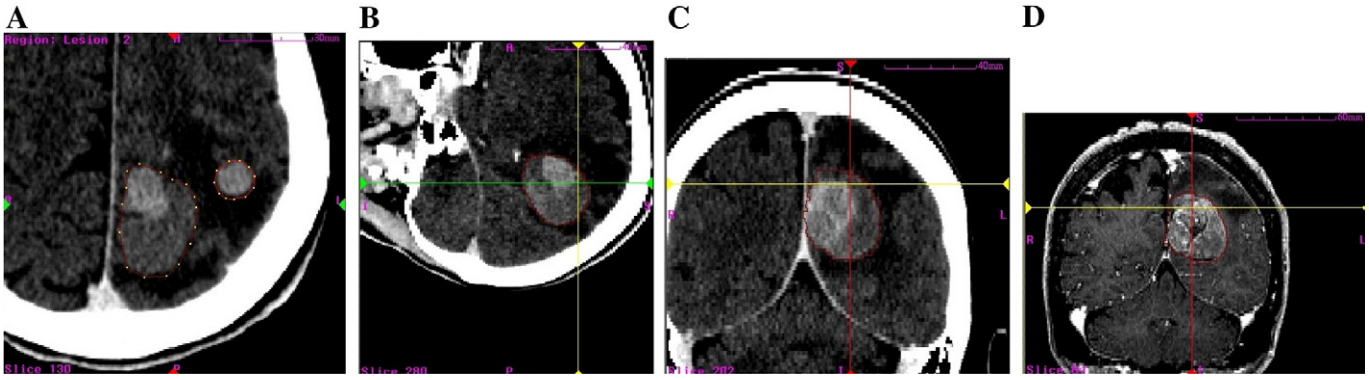

Fig. 1. (A) Axial CT scan view of both lesions. (B) Sagittal CT scan view of the bigger lesion that was operated on. (C) Coronal CT scan view of the brain tumor. (D) Coronal MRI + contrast (gadolinium) view of the bigger lesion that was operated on.

Additionally, blood flow can be delineated by IR thermography (Watson et al., 2002) and was appearing to be lower in primary brain tumors than in normal tissue (McCulloch, 1984).

Major factors that can contribute to hypothermia are reported as following:

a) Low density in tumor microvessels (Gorbach et al., 2004; Ecker et al., 2002);
b) Edema in the surrounding tissues due to the growth of the tumor, which increases the volume of white matter (Gorbach et al., 2004; Ecker et al., 2002);
c) Lower metabolism in the cortex overlying intracranial tumors is due to "Disconnection Effect" caused by edema (Gorbach et al., 2004; Ecker et al., 2002);
d) Tumor necrosis, which is typically caused by significant reduction of tumor vasculature or metabolic activity.

All these factors may cause reduction in Cerebral Blood Flow (CBF), metabolic activity or both. This, in turn, lowers the temperature in brain tumors. However, great levels of biological diversity in the tumor may contribute to fluctuation of temperature throughout tumors. A tumor with a mixture of higher and lower temperatures has been documented (Gorbach et al., 2004).

The purpose of this case study is to evaluate the thermal profile of a metastatic melanoma tumor in respect to its surrounding tissue in a 76-year-old Caucasian female patient. Additionally, it seeks to further investigate the usefulness of thermal imaging as an additional intraoperative modality and compare the gathered data with what is already reported in the literature.

Case report

History and presentation

We are reporting a 76-year-old Caucasian female patient who was presented with a long history of melanoma. She came to our clinic to treat her metastatic brain tumor. The patient was followed for melanoma for the past several years. CT and MRI with and without contrast were performed on the patient, which identified two lesions in the left posterior frontal and anterior parietal regions, consistent with malignant melanoma metastasis (Figs. 1 and 2). Surgical resection of the larger of the two lesions was recommended. The large lesion was causing a mass effect, had actually grown despite Gamma Knife radiosurgery and thus had to be surgically removed. A second, smaller lesion in a more eloquent area was treated with Gamma Knife.

There are three sets of images used in this study: pre-resection CT, pre-resection MR and post-resection MR images. These MRI and CT data sets of the patient were obtained at the imaging facilities of the University of Southern California (USC) University Hospital. A complete pre-resection CT image data set (176 slices, 512×512 pixel matrix) with a 1.5 mm thickness and zero gap in the transverse plane was acquired with a Philips MX 8000 IDT scanner (Philips Medical System, Shelton, CT). The field of view was 300×300 mm^2.

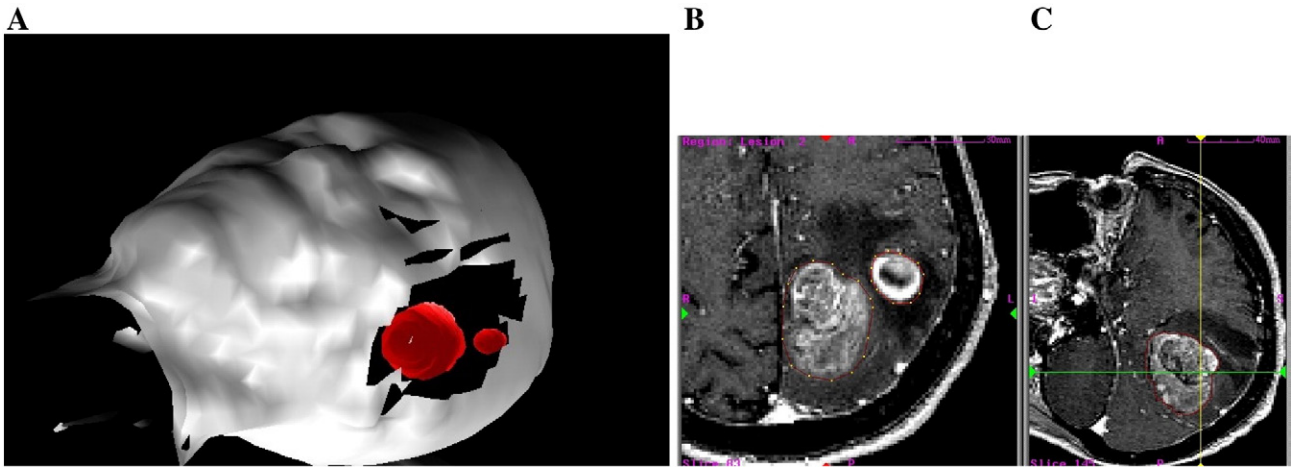

Fig. 2. Pre-op volumetric measurement of both lesions based on the CT and Stealth MRI: the larger lesion had the volume of 44.6 cc while the smaller lesion volume was 4.3 cc.

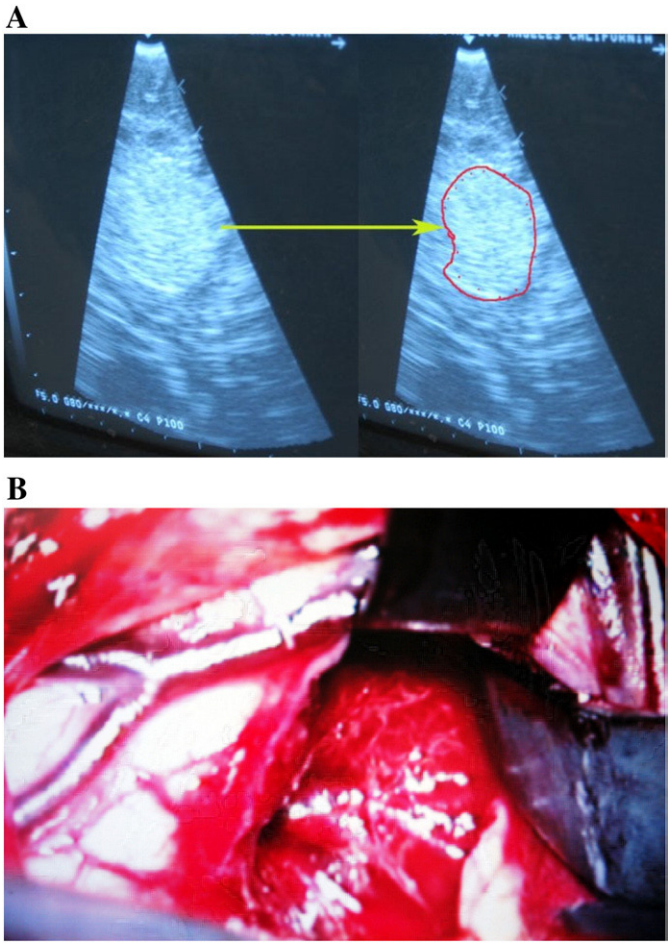

Fig. 3. A and B are demonstrating the intra-operative ultrasound of the larger lesion and the real-time picture of the intra-cortical melanoma prior to the gross complete resection.

The CT images were originally acquired for a CyberKnife™ (Accuray Inc., Sunnyvale, California) radiosurgery procedure. The image data set was transferred through the hospital network system to the CyberKnife Treatment Planning System (version 3.2.0.2), where the delineation and calculation of lesions were performed. Both pre- and post-resection MRI acquisitions were done with a Philips Gyroscan, 1.5 T MRI scanner (Philips Medical System, Shelton, CT). The T1-weighted imaging sequences (256×256 pixel matrix) with a 1.5 mm thickness and zero gaps were acquired in transverse. The field of view was 250×250 mm^2. The repetition time was 620 ms with an echo time of 20 ms. Pre-resection MR images of 176 slices were acquired without the head frame or fiducials. These images were transferred through the hospital network system to the CyberKnife Treatment Planning System, where the delineation and calculation of lesions were performed. Post-resection MR images were acquired for the Gamma Knife stereotactic radiosurgery. The delineation and calculation of lesion volume were done with the Leksell GammaPlan software system (LGP version 5.33, Elekta, Norcross, GA).

Operative report

After placement of stealth localizing fiducials on the head, the patient was first taken to the MR scanner where a Stealth MR was obtained (Figs. 1D, 2B and C). The patient was then taken back to the OR, where the fiducials were registered on the Stealth MRI and then the point of optimal incision was determined using the Stealth guidance. Ultrasound was used to verify the location of the tumor with respect to the dural surface (Fig. 3A) as well as localize the tumor prior to making a corticectomy in the middle of the exposed cortical surface.

The FLIR Systems' TCP60 infrared thermal camera was used to record the thermal profile of the surgical field prior to and following tumor resection. TCP60 utilizes a fourth generation 320×240 uncooled micro-barometer Focal Plane Array (FPA) detector, which provides high spatial resolution (7.5 to 13 μm) with a thermal sensitivity of 0.06 °C at an ambient recording temperature of 30 °C. Thermal images were recorded after the initial exposure of the tumor (Figs. 4A and B) and after resection (Figs. 6B and C). These images were visually compared to the pre- and post-resection Stealth MRI (Fig. 2). The images were used for reconstructuring the 3D volumetric measurement of the tumor. The same images were used for the CT scan (Fig. 5B) to measure operative volume of residual tumor/blood. Additionally, intraoperative ultrasound was used (Fig. 3A) to determine accuracy of the tumor margin data obtained from the camera.

The Stealth MRI was once again used to estimate the depth of the lesion. Next, under microscopic guidance, the tumor was carefully removed from the surrounding white matter. Tumor margins were delineated using the ITI. We assessed and compared the margins obtained based on MRI with the intraoperative ultrasound and light microscopy. Once the entire resection bed was exposed, the tumor resection cavity was irrigated and a single layer of Surgicel was placed to stop any oozing. The intraoperative impression based on light

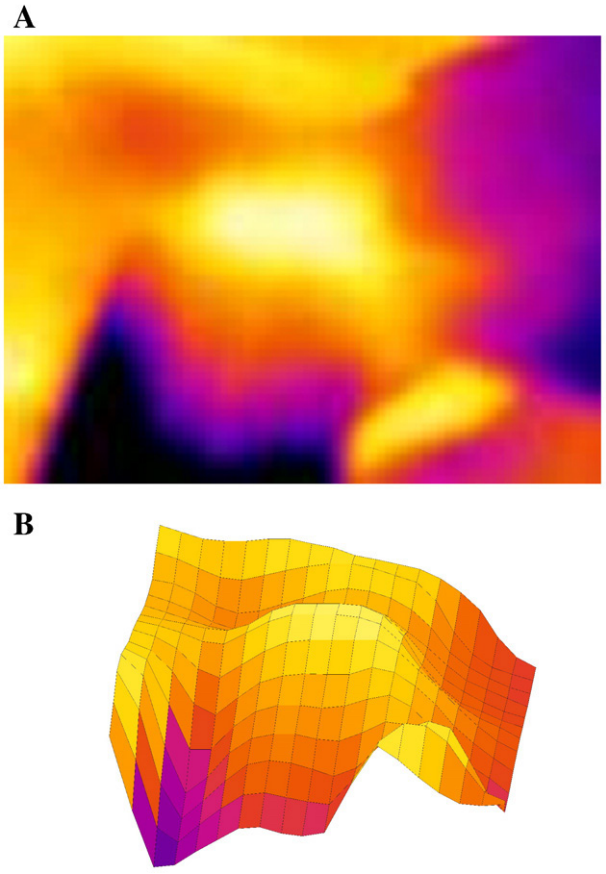

Fig. 4. (A) shows a pre-operative co-localization of brain tumor mass and margin using intraoperative thermal imaging. View of the tumor before the attempt for gross total resection. (B) A 3D pre-op Intraoperative Thermal Imaging of the tumor. Please pay attention to the higher (white area, 36.4 °C) temperature recording versus normal soundings (yellow, 33.1–5 °C, based on the blood flow).

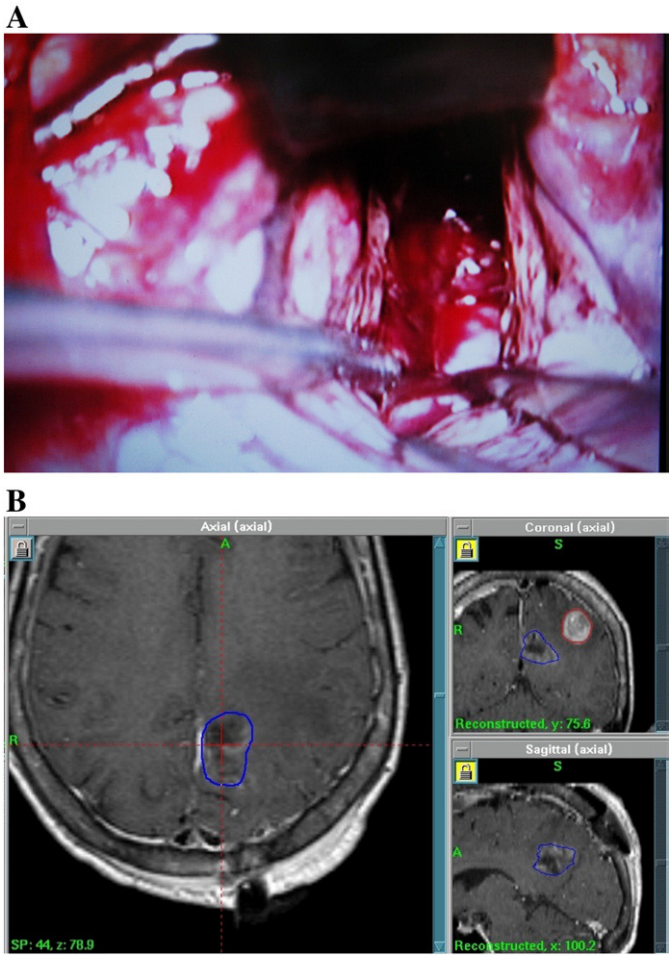

Fig. 5. (A) represents the tumor cavity right after resection and removal of the Surgicel. Please note the blood at the floor of the tumor resection cavity. (B) A post resection MR + contrast reveals high signal areas at the floor of tumor resection cavity, which was confirmed in the radiology report as blood and residual microscopic tumor.

microscopy observation suggested that the tumor was completely resected.

Results

Analysis of the technical report

In this study, we hypothesized that temperature gradients, arising possibly due to variations in metabolic pathways or vasculature in patients with intracortical melanoma, could be detected by ITI. To further investigate the validity of our hypothesis, we used the TCP60 (FLIR systems) intra-operatively and in parallel with CT, MRI, Ultrasound, CyberKnife and Gamma Knife. Fig. 2 shows a pre-resection volumetric measurement of both brain tumor lesions based on the CT and MRI (larger lesion: 44.6 cc; smaller lesion: 4.3 cc), calculated using Stealth MRI and CyberKnife.

Figs. 3A and B show the intraoperative ultrasound of the brain tumor and the real-time picture of the intracortical melanoma prior to the gross complete resection. The ultrasound and the gross picture of the melanoma revealed a highly vascularized intracortical mass with semi-distinctive margins.

Fig. 4 shows a pre-resection co-localization of brain tumor mass and margin using ITI (A), which also demonstrates a view of the tumor before the gross total resection. The tumor is clearly demarcated by a higher temperature (36.4 °C) in respect to the surrounding normal tissue (33.1–5 °C). There were three other hyperthermia areas on the pia mater facing the camera. These hyperthermic areas were initially thought to be background noise. However, after background noise elimination, we continued to observe such hyperthermic areas from the pia away from the blood vessels. Fig. 4B represents a pre-resection ITI of the tumor (3D plot), which demonstrates a higher (white area, 36.4 °C) temperature recording versus normal surroundings (yellow, 33.1–5 °C, based on the blood flow). Graph 1 shows a pre-resection thermal fingerprint of the tumor and its margin in respect to the retractors (landmark). The highest temperature recorded in this graph is 36.4 °C–33.5 °C versus 33.1–33.5 °C for normal cortical recording. It is important to note that in the OR, the surface of the brain is usually cooler by about 4 °C than the normal physiological temperature (37 °C), because the OR room temperature is much lower (at around 19 to 20 °C) than body core temperature. Thus, cooler OR temperature will have an impact on the ITI recording before the brain is exposed surgically.

Figs. 5A and B represent the tumor cavity immediately after gross resection and removal of the Surgicel. The blood at the floor of the tumor resection cavity is noticeable.

A post-resection MR + contrast reveals high signal areas at the floor of tumor resection cavity, which could be either residual blood or microscopic tumor or both. Fig. 6A shows a 3-dimensional CT-based Gamma Knife reconstruction of the two lesions, which was done post-resection. The figure shows a volumetric estimate of the enhanced area, 7.3 cc residual, which is thought to be blood and/or tumor. We thus estimate that 83.6% of the brain tumor was removed by near total resection and 16.4% of residuals could be visualized using thermal imaging, which could not be seen with the intraoperative microscope.

As it was mentioned earlier, the second lesion was treated with a Gamma Knife radiosurgery. Fig. 6B represents a post-resection thermal imaging of the tumor resection cavity, which demonstrates near total resection of the metastasis with some enhancement at the floor of the tumor cavity.

Fig. 6C shows a 2D thermal profile of the tumor. Black edges of the profile are representing the areas in which IR was blocked due to a presence of water or body fluid (i.e. blood). Post-resection thermal profile of the tumor resection cavity indicated that there may be an existence of residual tumor (Graph 2).

Discussion I: technology

Heat emission in the infrared (IR) range is a known physical property of all objects including the biological tissues, which correlates with the temperature of the matter (Wein's Law). Electromagnetic waves in the IR range (3–5 μm for mid wavelength IR and 8–14 for long wavelength IR) easily travel through the atmosphere at the speed of light and can be detected as a photons or quanta of energy (Shevelev et al., 1998). These physical properties make it easy to detect the thermal or IR emission of an object, in this case a biological specimen or tissue, from a distance using a sensitive lens (Shevelev et al., 1998). However, IR waves are absorbed by fluid and glass. Thus, the surgical field must be dried before application of ITI.

Technologically, TCP60 can capture the infrared emission spectrum of a relatively large clinically relevant field at once. A Windows-based software tool allowed real-time analysis and display of the captured infrared emissions and their corresponding temperatures. The spatial resolution of the camera is 7.5–13 μm. The thermal sensitivity of the camera is 0.06 °C, which is a significant improvement over other intraoperative visible microscopy imaging. However, thermal imaging is a surface recording of the heat profile of an object with low penetration. Thus, the use of ITI requires clear exposure of the lesion. The surface temperature data set is an additional intraoperative tool for analysis of the surgical field that can delineate neoplasms and their margins. This is especially valuable because of the limitations of current neuroimaging techniques such as CT and

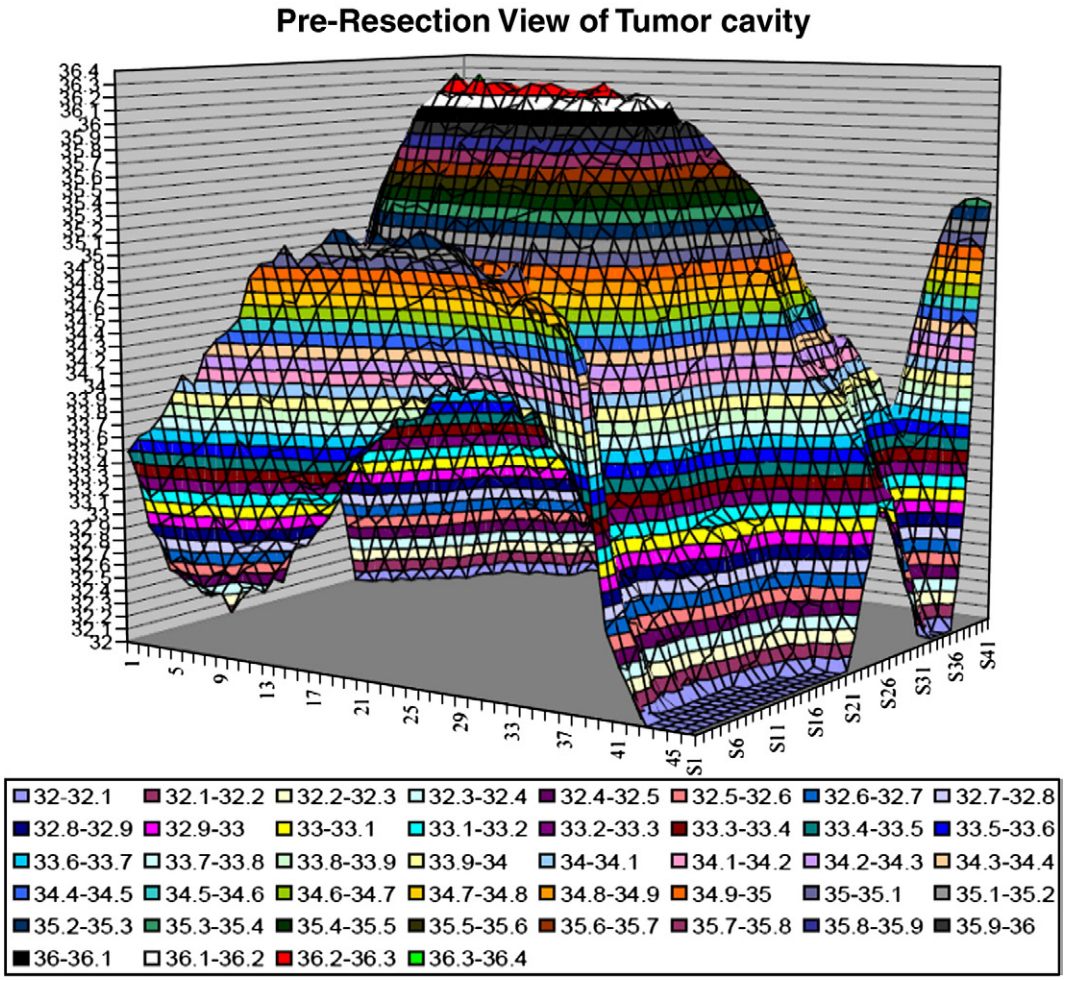

Graph 1. A pre-resection fine thermal fingerprint of the tumor and its margin. Please note that the cortical recording of 33.1–5 °C was used as a control in this case.

MRI. One of such limitation is that when contrast is used in CT, the volume of tumor may be greater than what the contrast indicates (Burger et al., 1988; Kelly et al., 1987). Moreover, the area of contrast enhancement may be a more of an assessment of abnormal blood brain barrier (BBB) than of tumor margin (Burger et al., 1988; Nazzaro and Neuwelt, 1990). Tumor can also extend past areas of hypodensity on CT (Nazzaro and Neuwelt, 1990; Burger et al., 1988). In MRI, true tumor margins can extend beyond the area of abnormal signal (Kelly et al., 1987). Differentiation between tumor and surrounding edema is difficult (Holland et al., 1985). Like CT, a contrast enhanced MRI is also subject to variances in BBB permeability at the margins of tumor. Additionally the resolution of 1.5 T MRI, the most common MRI technology currently used, is only 256×256 pixels versus 340×240 pixels for ITI.

Although recent advancements in MRI and CT scan technology offers higher resolution and precision of brain images (Shi et al., 1993), determination of pre- and post-resection volumes of tumors using MRI are of limited intraoperative value. These imaging modalities are still non-dynamic with respect to intraoperative changes of brain topography and tumor dimensions due to intraoperative debulking and manipulations. While the bulk of the tumor can be removed by gross visual inspection, an accurate visual assessment of some tumor margins is extremely difficult. Moreover, the use of pathological specimens to confirm tumor margins could be time consuming, since the biopsy needs to be taken point-by-point and staining takes long time on numerous biopsies. Thus, there is a great need for development of new multimodality intraoperative optical imaging technologies that could assess the margin as well as biological nature of the tumors.

Discussion II: feasibility of thermal imaging as an intraoperative tool

Brain metastasis is much more common than primary brain tumors as an estimated 20 to 40% of cancer patients will eventually develop metastatic brain tumors. Metastatic brain tumor has an incidence of more than 100,000 cases per year in the United States alone (ABTA Facts and Statistics, 2008; Nathoo et al., 2004; Tan and Black, 2003). Metastatic melanoma in the brain accounts approximately 5 to 10% of all metastasis to the brain and the third most common metastasis to the brain after lung and breast cancers (Nathoo et al., 2004). Melanomas in the brain are known to induce intracranial hemorrhage and often invade vasculature (Byrne et al., 1983). Previous published data indicated that metastatic brain tumors, including intracortical melanoma, exhibited hyperthermic profiles (Gorbach et al., 2004; Ecker et al., 2002). Interestingly, thermography has been used to investigate melanoma and consistently reported that it was hyperthermic. The first experimentation on cutaneous malignant melanoma was conducted in 1964 and revealed a hyperthermic profile with respect to surrounding normal tissue (Di Carlo, 1995). Subsequent studies revealed similar findings. These studies have established that thermography is a reliable detection and prognostic (Michel et al., 1985) tool in cutaneous melanoma diagnosis. In addition to the dermatological application of TES, corneal and ocular malignant melanomas have also been detected using IR

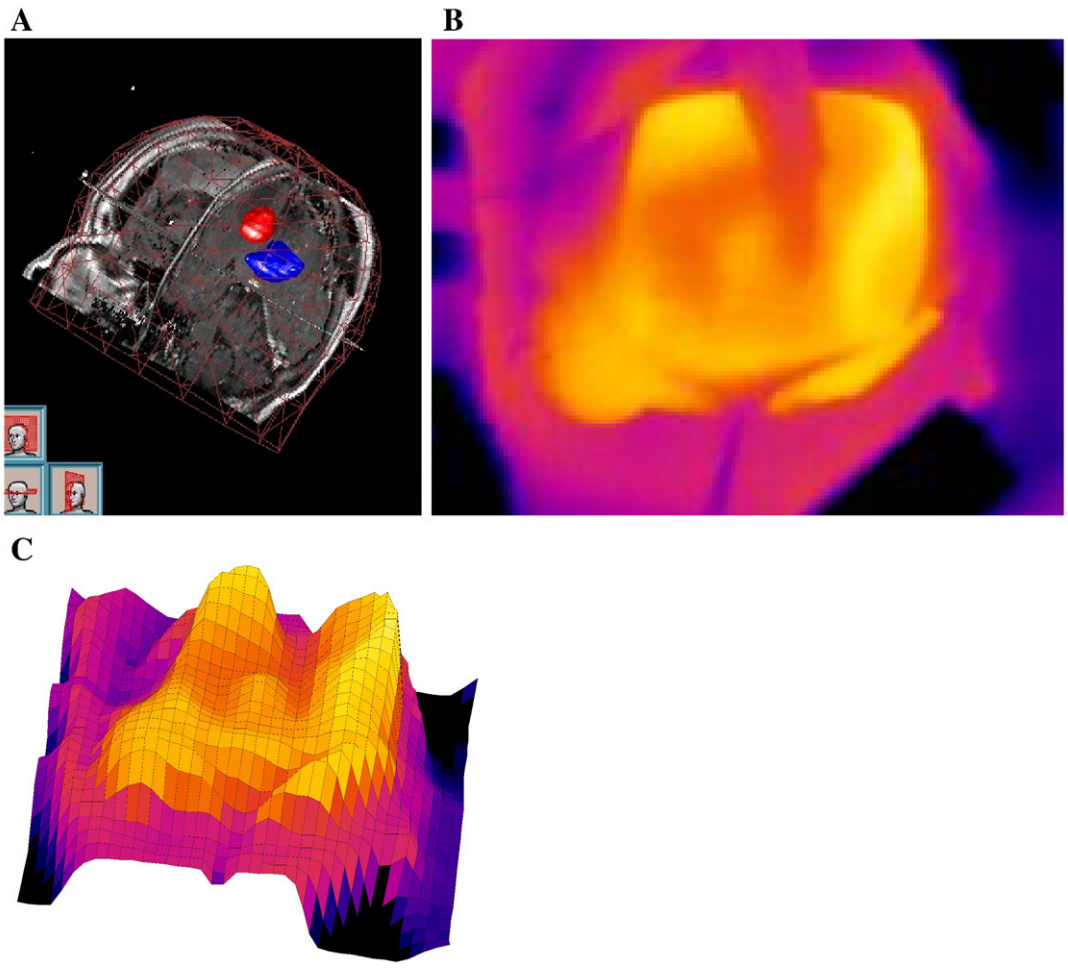

Fig. 6. (A) represents 3D CT based Gamma Knife reconstruction of the two lesions, post-resection, which accurately estimates the volumetric measurement of the enhanced area, 7.3 cc residuals (blood/tumor). The second lesion was treated with Gamma Knife. (B) is a post-resection thermal imaging of the tumor resection cavity, which demonstrates near total resection of the metastasis. (C) represents a 3D thermal profile of the tumor after resection. Note the black edges of the profile as they represent areas, which IR was blocked due to the presence of water or body fluid (blood).

thermography. Like cutaneous melanomas and the tumor in this case report, these tumors displayed a hyperthermic profile with respect to the surrounding normal tissue (Wittig et al., 2002).

In this case study, we have confirmed the observation by Gorbach et al. (2004) that metastatic brain tumors are generally hyperthermic. The radiology report in this case has also confirmed the existence of post-resection tumor residual as well as blood in the brain tumor resection cavity.

Neural activity, local metabolism, blood flow, and thermal conductivity are significant factors that contribute to the thermal profile of a tissue (Michel et al., 1985). Our results concur with previous efforts to characterize the thermal profile of malignant melanoma in other locations of the body. Whether this hyperthermic profile is inherent to malignant melanomas regardless of location remains to be seen. These studies may further assist in demarcating the margins of brain tumors with increased confidence and accuracy so that tumors can eventually be resected at their margins with extreme precision even in metastasis. This technology could make the process more objective and provide surgeons with additional tools to achieve complete resection, which is proven to have a positive impact on the survival of patient with intracranial mass (Sanai and Berger, 2008; McGirt et al., 2009).

Our study, as well as the literature, suggests that thermal imaging can provide the neurosurgeons with additional information to demarcate tumors and possibly some residual tumors (Gorbach et al., 2004). In addition, ITI can continuously monitor pathological vascular condition and assess function of adjacent tissues during surgery. ITI is cost-efficient, non-invasive, and can be used in patients whose conditions do not allow us to use intraoperative-MRI (such as having implants, etc.) and thus is potentially very versatile, useful intraoperative tool. Current software programs or algorithms, however, cannot detect tumor margins clearly and automatically to allow surgeons to use ITI as a definitive tool to delineate tumor borders. The limitations of this technology include: 1) lack of software that could auto-delineate the tumor margin, 2) higher resolution camera than what we used in this case report is needed for the future studies and 3) less than 0.5 mm IR penetration depth.

Conclusions

Intraoperative IR imaging holds a great promise, as shown in this paper as an alternative, non-invasive, and cost-efficient imaging method to assist surgeons in identifying tumor location, and to potentially detect vasculature and other acute abnormalities on the spot during the surgery. Data derived from more extensive human studies will allow us to better understand brain tumors and to eventually use this technique at the time of surgery as an imaging aid for the removal of brain tumors. Ultimately, with advancement in camera, instruments, and analysis software programs, infrared thermography could be part of a new generation of high-resolution

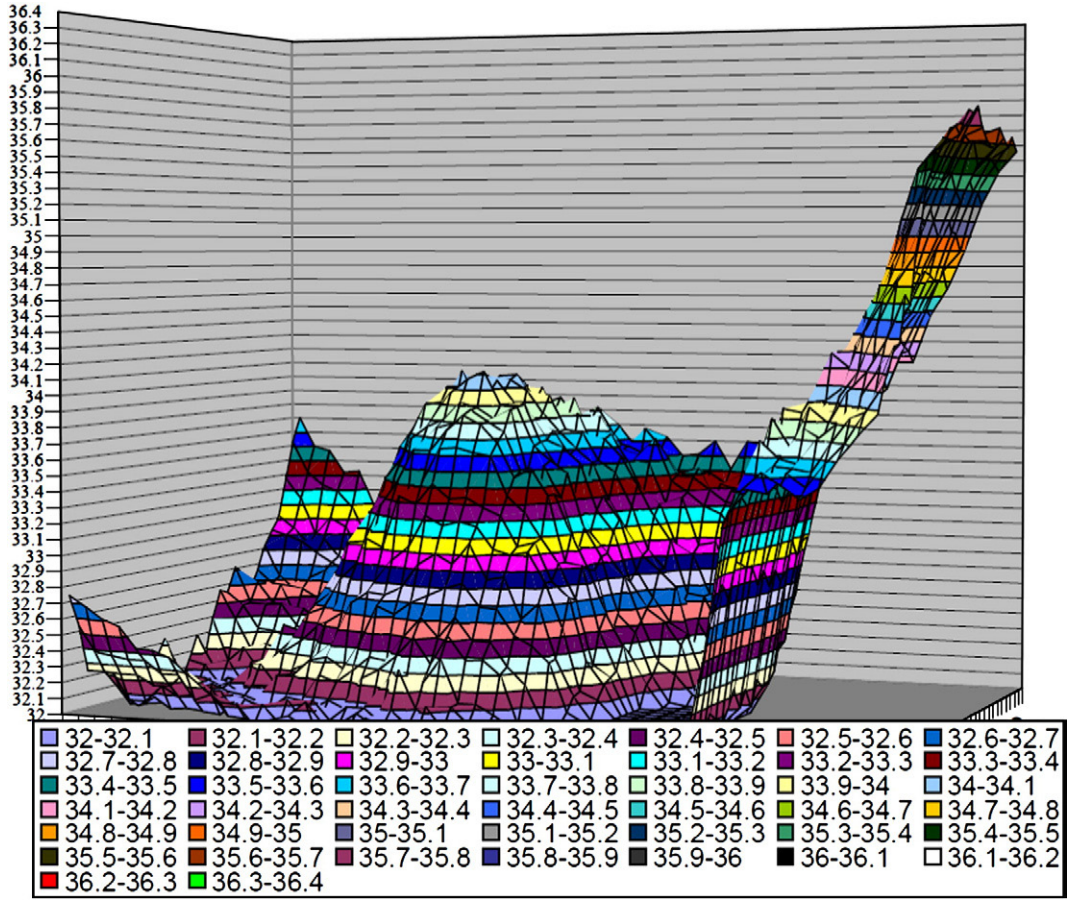

Graph 2. Post-resection thermal profile of the tumor resection cavity, which reveals a presence of a residual mass. This could be either blood or tumor. The normal cortical temperature recorded in this patient was 33.1–5 °C. In this case the highest temperature recorded at the floor of the tumor cavity was 34.1 °C. There is no thermal profile of metallic retractors appearing on this graph. The radiology report in this case has also confirmed existence of post resection tumor residual as well as blood in the tumor resection cavity.

neurosurgical microscopes that can distinguish between normal and neoplastic tissue with exceptional precision using other multimodality biophotonic technologies.

Conflict of interest statement
The authors declare there is no conflict of interest.

Acknowledgments

We would like to thank Mr. Brad Risser, FLIR system, who provided us with the TCP60. This project could not be possible without the significant administrative and technical assistance of professors Martin Weiss, Steven Geonnatta, Dr. Darcy Spicer (chair of the IRB committee) and Dr. Crohen (the anesthesiologist). We thank Dr. Payman Moin for his logistical assistant and Dr. Sean MacNatt for helping Dr. Gruen in the surgery. We also thank Dr. Ilya Eckstein for his editorial comments. This work is made possible by Brain Mapping Foundation and International Brain Mapping and Intraoperative Surgical Planning Society (www.IBMISPS.ORG).

Appendix A. Supplementary data

Supplementary data associated with this article can be found, in the online version, at doi:10.1016/j.neuroimage.2009.03.043.

References

ABTA, 2008 ABTA (American Brain Tumor Association). "Facts & Statistics, 2008" www.abta.org.

Arora, N., Martins, D., Ruggerio, D., Tousimis, E., Swistel, A.J., Osborne, M.P., Simmons, R.M., 2008. Effectiveness of a noninvasive digital infrared thermal imaging system in the detection of breast cancer. Am. J. Surg. 196 (4), 523–526.

Barrett, A.H., Myers, P.C., Sadowsky, N.L., 1980. Microwave thermography in the detection of breast cancer. AJR, Am. J. Roengenol. 34 (2), 365–368.

Black, P.M., Moriarty, T., Alexander 3rd, E., Stieg, P., Woodard, E.J., Gleason, P.L., Martin, C.H., Kikinis, R., Schwartz, R.B., Jolesz, F.A., 1997. Development and implementation of intraoperative magnetic resonance imaging and its neurosurgical applications. Neurosurgery 41 (4), 831–842.

Burger, P.C., Heinz, E.R., Shibata, T., Kleihues, P., 1988. Topographic anatomy and CT correlations in the untreated glioblastoma multiforme. J. Neurosurg. 68, 698–704.

Byrne, T.N., Cascino, T.L., Posner, J.B., 1983. Brain metastasis from melanoma. J. Neuro-Oncol. 1, 313–317.

DeAngelis, L.M., 2001. Brain tumors. N. Engl. J. Med. 344, 114–123.

Di Carlo, A., 1995. Thermography and the possibilities for its applications in clinical and experimental dermatology. Clin. Dermatol. 13, 329–336.

Ecker, R.D., Goerrss, S.J., Meyer, F.B., Cohen-Gadol, A.A., Britton, J.W., Levine, J.A., 2002. Vision of the future: initial experience with real-time intraoperative high-resolution Dynamic Infrared Imaging (DIRI). J. Neurosurg. 97 (6), 1460–1471.

Fahlbusch, R., Samii, A., 2007. A review of cranial imaging techniques: potential and limitations, clinical neurosurgery. Congress Neurol. Surg. 54 (17), 100–104.

Frangioni, J.V., 2008. New technologies for human cancer imaging. J. Clin. Oncol. 26 (24), 4012–4021.

Gonzalez, F.J., (2007). Infrared Imager Requirements for Breast Cancer Detection. Proceedings of the 29th Annual Int'l Conference of the IEEE EMBS. 3312–3314.

Gorbach, A.M., 1993. Infrared imaging of brain function. Adv. Exp. Med. Biol. 333, 95–123.

Gorbach, A., Simonton, D., Hale, D.A., Swanson, S.J., Kirk, A.D., 2003. Objective, real-time, intraoperative assessment of renal perfusion using infrared imaging. Am. J. Transplant. 3 (8), 988–993.

Gorbach, A.M., Heiss, J.D., Kopylev, L., Oldfield, E.H., 2004. Intraoperative infrared imaging of brain tumors. J. Neurosurg. 101, 960–969.

Gorbach, A.M., Wang, H., Dhanani, N.N., Gage, F.A., Pinto, P.A., Smith, P.D., Kirk, A.D., Elster, E.A., 2008. Assessment of critical renal ischemia with real-time infrared imaging. J. Surg. Res. 149 (2), 310–318.

Hadani, M., Spiegelman, R., Feldman, Z., et al., 2001. Novel, compact, intraoperative magnetic resonance imaging-guided system for conventional neurosurgical operating rooms. Neurosurgery 48, 799–809.

Hall, W.A., Truwit, C.L., 2008. Intraoperative MR-guided neurosurgery. J. Magn. Reson. Imaging 27 (2), 368–375 Feb.
Hall, W., Liu, H., Martin, A.J., et al., 2000. Safety, efficacy, and functionality of high-field strength interventional magnetic resonance imaging for neurosurgery. Neurosurgery 46, 632–642.
Head, J.F., Wang, F., Lipari, C.A., Elliot, R.L., 2000. The important role of infrared imaging in breast cancer. IEEE Eng Med. Biol. Mag. 19 (2), 52–57.
Hill, D., Maurer, C., Maciunas, R., Barwise, J., Fitzpatrick, J., Wang, M., 1998. Measurement of intraoperative brain surface deformation under a craniotomy. Neurosurgery 43 (3), 514–526.
Holland, B.A., Brant-Zawadzki, M., Norman, D., Newton, T.H., 1985. Magnetic resonance imaging of primary intracranial tumors: a review. Int. J. Radiat. Oncol. Biol. Phys. 11, 315–321.
Jiang, L.J., Ng, E.Y., Yeo, A.C., Wu, S., Pan, F., Yau, W.Y., Chen, J.H., Yang, Y., 2005. A perspective on medical infrared imaging. J. Med. Eng. Technol. 29 (6), 257–267.
Knauth, M., Wirtz, C., Tronnier, V., Aras, N., Kunze, S., Sartor, K., 1999. Intraoperative MR imaging increases the extent of tumor resection in patients with high-grade gliomas. Am. J. Neuroradiology 9, 1642–1646.
Kelly, P.J., Daumas-Duport, C., Scheithauer, B.W., Kall, B.A., Kispert, D.B., 1987. Stereotactic histologic correlations of computed tomography- and magnetic resonance imaging-defined abnormalities in patients with glial neoplasms. Mayo Clinic Proceeding 62, 450–459.
Konerding, M.A., Konerding, M.A., Fait, E., Dimitropoulou, C., Malkusch, W., Ferri, C., Giavazzi, R., Coltrini, D., Presta, M., 1998. Impact of fibroblast growth factor-2 on tumor microvascular architecture. A tridimensional morphometric study. Am. J. Pathol. 152 (6), 1607–1616.
Laws, E.R., Shaffrey, M.E., Morris, A., Anderson Jr, F.A., 2003. Surgical management of intracranial gliomas—does radical resection improve outcome? Acta Neurochir. Suppl. 85, 47–53.
Lindner, D., Trantakis, C., Renner, C., Arnold, S., Schmitgen, A., Schneider, J., Meixensberger, J., 2006. Application of intraoperative 3D ultrasound during navigated tumor resection. Minim. Invasive Neurosurg. 49 (4), 197–202.
McCulloch, J., 1984. Perivascular nerve fibres and the cerebral circulation. Trends Neurosci. 7, 135–138.
McGirt, M.J., Chaichana, K.L., Gathinji, M., Attenello, F.J., Than, K., Olivi, A., Weingart, J.D., Brem, H., Quiñones-Hinojosa, A.R., 2009. Independent association of extent of resection with survival in patients with malignant brain astrocytoma. J. Neurosurg. 110 (1), 156–162.
Merla, A., Romani, G.L., 2006. Functional infrared imaging in medicine: a quantitative diagnostic approach. Conf. Proc. IEEE Eng. Med. Biol. Soc. 1, 224–227.
Michel, U., Hornstein, O.P., Schonberger, A., 1985. Infrared thermography in malignant melanoma. Diagnostic potential and limits [in German]. Hautarzt 36, 83–89.
Mineo, J.F., Quintin-Roue, I., Lucas, B., Buburusan, V., Besson, G., 2002. Glioblastomas: clinical study and search for prognostic factors [in French]. Neurochirurgie 48, 500–509.
Mital, M., Scott, E.P., 2007. Thermal detection of embedded tumors using infrared imaging. J. Biomech. Eng. 129, 33–39.
Mitchell, P., Ellison, D.W., Mendelow, A.D., 2005. Surgery for malignant gliomas: mechanistic reasoning and slippery statistics. Lancet Neurol. 4, 413–422.
Mittal, S., Black, P.M., 2006. Intraoperative magnetic resonance imaging in neurosurgery: the Brigham concept. Acta Neurochir. Suppl. 98, 77–86.
Nabavi, A., Black, P.M., Gering, D.T., Westin, C.F., Mehta, V., Pergolizzi Jr, R.S., Ferrant, M., Warfield, S.K., Hata, N., Schwartz, R.B., Wells 3rd, W.M., Kikinis, R., Jolesz, F.A., 2001. Serial intraoperative magnetic resonance imaging of brain shift. Neurosurgery 48 (4), 787–797.
Nakagawa, A., Fujimura, M., Arafune, T., Sakuma, I., Tominaga, T., 2008. Intraoperative infrared brain surface blood flow monitoring during superficial temporal artery–middle cerebral artery anastomosis in patients with childhood moyamoya disease. Childs Nerv. Syst. 24 (11), 1299–1305.
Nakao, N., Nakai, K., Itakura, T., 2003. Updating of neuronavigation based on images intraoperatively acquired with a mobile computerized tomographic scanner: technical note. Minim. Invasive Neurosurg. 46 (2), 117–120.
Nathoo, N., Toms, S.A., Barnett, G.H., 2004. Metastases to the brain: current management perspectives. Expert Rev. Neurotherapeutics 4 (4), 633–640.
Nazzaro, J.M., Neuwelt, E.A., 1990. The role of surgery in the management of supratentorial intermediate and high-grade astrocytomas in adults. J. Neurosurg. 73, 331–344.
Nishikawa, K., Matsudaira, H., Suzuki, H., Mizuno, R., Hanyuu, N., Iwabuchi, S., Yanaga, K., 2006. Intraoperative thermal imaging in esophageal replacement: its use in the assessment of gastric tube viability. Surg. Today 36 (9), 802–806.
Papaioannou, T., Thompson, R.C., Kateb, B., Sorokoumov, O., Grundfest, W.S., Black, K.L., 2002. Thermal imaging of brain tumors in a rat glioma model. Proc. SPIE 4615, 32 DOI:10.1117/12.466653.
Rasmussen, I.A., Lindseth, F., Rygh, O.M., Berntsen, E.M., Selbekk, T., Xu, J., Nagelhus Hernes, T.A., Harg, E., Haberg, A., Unsgaard, G., 2007. Functional neuronavigation combined with intra-operative 3D ultrasound: initial experiences during surgical resections close to eloquent brain areas and future directions in automatic brain shift compensation of preoperative data. Acta Neurochir. 149, 365–378.
Reinertsen, I., Descoteaux, M., Siddiqi, K., Collins, D.L., 2007. Validation of vessel-based registration for correction of brain shift. Med. Image Anal. 11 (4), 374–388.
Samaras, C.A., Greenblatt, R.B., 1983. The role of thermography in breast cancer. Contemp. Surg. 22, 31–38.
Sanai, N., Berger, M.S., 2008. Glioma extent of resection and its impact on patient outcome. Neurosurgery 62 (4), 753–766.
Saxena, A.K., Willital, G.H., 2008. Infrared thermography: experience from a decade of pediatric imaging. Eur. J. Pediatr. 167, 757–764.
Schulder, M., Carmel, P.W., 2003. Intraoperative magnetic resonance imaging: impact on brain tumor surgery. Cancer Control 10 (2), 115–124.
Schulder, M., Liang, D., Carmel, P.W., 2001. Cranial surgery navigation aided by a compact intraoperative magnetic resonance imager. J. Neurosurg. 94, 936–945.
Shevelev, I.A., 1992. Temperature topography of the brain cortex: thermoencephaloscopy. Brain Topogr. 5, 77–85.
Shevelev, I.A., 1998. Functional imaging of the brain by infrared radiation (thermoencephaloscopy). Prog. Neurobiol. 56, 269–305.
Shevelev, I.A., Tsicalov, E.N., Gorbach, A.M., Budko, K.P., Sharaev, G.A., 1993. Thermoimaging of the brain. J. Neurosci. Methods 46 (1993), 49–57.
Shi, W.M., Wildrick, D.M., Sawaya, R., 1993. Volumetric measurement of brain tumors from MR imaging. J. Neuro-Oncol. 37, 87–93.
Stupp, R., Mason, W.P., et al., 2006. Radiotherapy plus concomitant and adjuvant temozolomide for glioblastoma. N. Engl. J. Med. (10), 987–996.
Tan, T.C., Black, P.M., 2003. Image-guided craniotomy for cerebral metastases: techniques and outcomes. Neurosurgery 53 (1), 82–90.
Tempany, C., McNeil, B., 2001. Advances in biomedical imaging. JAMA 285 (5), 562–567.
Unsgaard, G., Rygh, O.M., Selbekk, T., Müller, T.B., Kolstad, F., Lindseth, F., Hernes, T.A., 2006. Acta Neurochir. 148 (3), 235–253.
Ueda, M., Sakurai, T., Kasai, K., Ushikubo, Y., Samejima, H., 1997. Localisation of sensory motor cortex during surgery by changes of cortical surface temperature after median nerve stimulation. Lancet 350 (9077), 561.
Watson, J.C., Gorbach, A.M., Pluta, R.M., Rak, R., Heiss, J.D., Oldfield, E.H., 2002. Real-time detection of vascular occlusion and reperfusion of the brain during surgery by using infrared imaging. J. Neurosurg. 96, 918–923.
Wen, P.Y., Kesari, S., 2008. Malignant gliomas in adults. N. Engl. J. Med. 5, 492–507.
Wittig, I., Kohlmann, H., Lommatzsch, P.K., Kruger, L., Herold, H., 2002. Static and dynamic infrared thermometry and thermography in malignant melanoma of the uvea and conjunctiva [in German]. Klinische Monatsblatter fur Augenheilkunde 201, 317–321.